Characterization of caspase-dependent and caspase-independent deaths in glioblastoma cells treated with inhibitors of the ubiquitin-proteasome system

Carmela Foti,[1] Cristina Florean,[1] Antonio Pezzutto,[1] Paola Roncaglia,[2] Andrea Tomasella,[1] Stefano Gustincich,[2] and Claudio Brancolini[1]

[1]Dipartimento di Scienze e Tecnologie Biomediche, Sezione di Biologia and MATI Center of Excellence Università degli Studi di Udine, Udine, Italy and [2]Neurobiology Sector, International School for Advanced Studies, AREA Science Park, Trieste, Italy

Abstract

The regulation of the necrotic death and its relevance in anticancer therapy are largely unknown. Here, we have investigated the proapoptotic and pronecrotic activities of two ubiquitin-proteasome system inhibitors: bortezomib and G5. The present study points out that the glioblastoma cell lines U87MG and T98G are useful models to study the susceptibility to apoptosis and necrosis in response to ubiquitin-proteasome system inhibitors. U87MG cells show resistance to apoptosis induced by bortezomib and G5, but they are more susceptible to necrosis induced by G5. Conversely, T98G cells are more susceptible to apoptosis induced by both inhibitors but show some resistance to G5-induced necrosis. No overt differences in the induction of Noxa and Mcl-1 or in the expression levels of other components of the apoptotic machinery were observed between U87MG and T98G cells. Instead, by comparing the transcriptional profiles of the two cell lines, we have found that the resistance to G5-induced necrosis could arise from differences in glutathione synthesis/utilization and in the microenvironment. In particular, collagen IV, which is highly expressed in T98G cells, and fibronectin, whose adhesive function is counteracted by tenascin-C in U87MG cells, can restrain the necrotic response to G5. Collectively, our results provide an initial characterization of the molecular signals governing cell death by necrosis in glioblastoma cell lines. [Mol Cancer Ther 2009;8(11):3140–50]

Introduction

Glioblastomas (GBM) are among the most lethal tumors. In particular, grade IV GBMs (WHO grade 4) are highly recalcitrant to radiotherapies and chemotherapies, exhibiting robust angiogenesis, resistance to apoptosis, and propensity to necrosis. Median survival is about 1 year from the time of diagnosis, and despite great efforts during the last decade, improvement in survival of patients has been modest (1, 2).

A large body of evidences has established that inhibition of the ubiquitin-proteasome system (UPS) promotes cancer cell death by apoptosis (3). Food and Drug Administration and European Medicine Agency approval of the UPS inhibitor (UPSI) bortezomib for the treatment of multiple myeloma has validated the UPS as a novel target in anticancer therapy (4). Isopeptidases are attractive alternative targets of the UPS for developing new antitumor therapies (5). Isopeptidases can be generally subdivided into deubiquitinating enzymes and ubiquitin-like (Ubl) specific proteases, which, respectively, deconjugate ubiquitin or Ubl molecules, such as SUMO, NEDD8, or ISG15, from target proteins. These enzymes modulate several biological processes through the control of the lifetime, localization, and activity of ubiquitin or Ubl-modified proteins (6, 7).

We have recently identified two new isopeptidase inhibitors, F6 and G5 (8). F6 and G5 inhibit isopeptidases by reacting with the sulfhydryl group of the catalytic cysteine (9). Because the vast majority of ubiquitin and Ubl proteases are cystein proteases (6), G5 and F6 are rather broad (nonselective) isopeptidase inhibitors (10).

G5, differently from bortezomib, can induce a necrotic death in cells resistant to apoptosis (11). Apoptosis resistance and susceptibility to necrosis are distinctive features of GBM (1). Hence, GBM cell lines represent the ideal model to investigate the pronecrotic activity of G5. In the present study, we have characterized the prodeath activities of bortezomib and G5 in two GBM cell lines and discovered the transcriptome differences that govern the necrotic susceptibility to G5.

Materials and Methods
Reagents

Information on antibodies and reagents is provided in Supplementary Data.

Cell Culture Conditions, Time-Lapse Analysis, Cell Death, and Retroviral Infection

Human GBM cell lines U87MG and T98G, tested by microarray analysis, were grown in DMEM supplemented with 10% fetal bovine serum, penicillin (100 U/mL), glutamine (2 mmol/L), and streptomycin (100 μg/mL) at 37°C in 5% CO_2 atmosphere. U87MG cells expressing mutant p53 and Bcl-xL were generated by retroviral infection (12), after cloning mutant *p53R175H* and *bcl-xL*, respectively, into pWZL-hygro and pWZL-Neo retroviral vectors.

For studying the role of extracellular matrix (ECM) on G5-induced necrosis plates were coated with fibronectin, collagen IV, or bovine serum albumin (10 μg/mL). Cells were seeded at 15×10^4/mL and were then allowed to adhere for 6 h at 37°C before treatments. In all trypan blue exclusion assays, 400 cells, from three independent samples, were counted for each data point.

Western Blotting

Proteins obtained after an SDS denaturating lysis and sonication were transferred to a 0.2-μm-pore-sized nitrocellulose membrane and incubated with the specific primary antibodies. After several washes, blots were incubated with peroxidase-conjugated goat anti-rabbit or goat anti-mouse (Euroclone Milano I) for 1 h at room temperature. Finally, blots were developed with Super Signal West Pico, as recommended by the vendor (Pierce).

RNA Expression Array and Data Analysis

Total RNA was isolated using TRIzol (Invitrogen) according to manufacturer's instructions, and purified with the RNeasy Mini kit (Qiagen). A 6-μg-amount of each total RNA sample was labeled according to the standard one-cycle amplification and labeling protocol (Affymetrix). Hybridization and analysis methods are detailed in the Supplementary Data.

Results

Death of GBM Cells in Response to G5 and Bortezomib

To study the prodeath activities of bortezomib and G5, we selected two GBM cell lines: T98G cells, mutated for p53, and U87MG cells, wild-type for p53 (13). Cells were treated with different concentrations of the drugs, and cell death was analyzed 20 hours later. Both compounds similarly induced the accumulation of polyubiquitinated proteins (data not shown).

Dose-dependent studies showed that U87MG cells are more prone to die in response to G5 compared with T98G cells (Fig. 1A). Incubation with 10 μmol/L of G5 elicited death in >90% of U87MG cells, whereas death was around 40% in T98G cells. In particular, in T98G cells, death was only marginally increased, despite dose escalation from 2.5 up to 10 μmol/L of G5. Surprisingly, bortezomib achieved an opposite effect. U87MG cells were more resistant to cell death (~30% of dead cells after incubation with 10 μmol/L of bortezomib), whereas T98G cells were more sensitive (>80% of death under the same conditions).

Next, we evaluated caspase-3 and caspase-7 activities (DEVDase). In cells treated with bortezomib, there is a perfect correlation between the DEVDase activity and the appearance of cell death (Fig. 1B). During the time of the analysis in the responsive T98G cells, bortezomib activates caspases and induces cell death, whereas in U87MG cells caspase activity is negligible.

In response to low doses of G5 (0.6 and 1.25 μmol/L), caspase activity parallels the induction of death in both cell lines (Fig. 1B). On the contrary, at higher doses of G5 (5 and 10μmol/L) that promptly kills U87MG cells, caspase activity declines.

To confirm the pattern of caspase activity, we investigated caspase-2 and HDAC4 proteolytic processing by immunoblots. As shown Fig. 1C and D, cleavages of HDAC4 and caspase-2 in response to different doses of G5 or bortezomib can be superimposed to the DEVDase activities shown in Fig. 1B. In particular, higher doses of G5 suppressed caspase-2 and HDAC4 processing in U87MG cells. Analogous results were acquired when caspase-3 processing was investigated by immunoblot (data not shown).

G5 Induces a Caspase-Independent Necrotic Death in Apoptosis-Resistant U87MG Cells

The progressive decline of caspase activities observed in U87MG cells treated with escalating doses of G5 is reminiscent of a caspase-independent necrotic death. To prove this hypothesis, we evaluated the ability of a pan-caspase inhibitor to influence death of U87MG and T98G cells in response to G5 or bortezomib.

The caspase inhibitor did not influence death of U87MG cells in response to G5, whereas cell death in response to bortezomib was partially impaired (Fig. 2A, *top*). In T98G cells, bortezomib-induced death was strongly affected by the caspase inhibitor, whereas death in response to G5 was inhibited to some extent (Fig. 2A, *bottom*). These results suggest that death in U87MG cells is prevalently caspase independent (necrotic), whereas in T98G cells it is prevalently caspase dependent (apoptotic).

Apoptosis in response to proteasome inhibition requires the synthesis of new proteins such as the BH3-only Noxa (3). Figure 2B shows that G5-induced death in T98G cells was inhibited by the protein synthesis inhibitor CHX, whereas the same treatment was ineffective in preventing death of U87MG cells. This result further suggests that G5 induces different types of death in U87MG and T98G cells.

High concentrations of the redox cycling quinone DMNQ can induce necrosis and kill cells mutated for Bax and Bak (11). G5 diverges from DMNQ because it can induce necrosis without eliciting oxidative stress. To understand whether U87MG cells are in general more prone to die by necrosis, we assessed cell death in response to DMNQ and G5 treatments. Figure 2C illustrates that U87MG cells are more prone to die in response to G5 compared with DMNQ, whereas T98G cells, on the opposite, are more prone to die in response to DMNQ. These data indicate that U87MG cells are highly susceptible to G5-induced necrosis but resistant to a redox-dependent necrotic insult.

Finally, the induction of necrosis in U87MG cells was unambiguously proved by time-lapse epifluorescence microscopy in living cells, which discriminates the appearance of necrosis, apoptosis, and secondary necrosis as a consequence of apoptosis (Supplementary Fig. S1).

Expression of Bcl-2 Family Members in Response to G5 or Bortezomib Treatments

The delicate balance among Bax and Bak proteins and their antagonists, Bcl-2, Bcl-xL, and Mcl-1, dictates the apoptotic susceptibility to UPSIs (3). Hence, we investigated Bcl-2, Bcl-xL, Mcl-1, Bax, and Bak levels in U87MG and T98G cells treated with bortezomib or G5. We also analyzed expression levels of direct (p53) and indirect (the BH3-only protein Noxa) targets of bortezomib and G5. Since certain Bcl-2 family members are cleaved and downregulated by caspases, as an effect of the amplificatory mechanisms (14), to avoid massive caspase activation, incubations were done for limited times and with low concentrations of G5 or bortezomib.

Overall Bcl-2, Bcl-xL, Bax, and Bak were similarly expressed in the two GBM cell lines (Fig. 3A). Only minor differences can be observed. Bak and Bcl-xL levels were increased in T98G cells, whereas Bcl-2 and Bax were augmented in U87MG cells. Mcl-1 and Noxa were similarly induced by G5 and bortezomib treatments in both cell lines, and as expected, p53 was stabilized only in U87MG cells, but here again at comparable levels by the two inhibitors.

The only exception concerned the downregulation of Bcl-xL levels in U87MG cells treated with G5. To prove whether the downregulation of Bcl-xL in response to G5 could be important for the manifestation of necrosis, cells overexpressing Bcl-xL were generated by retroviral infection (Fig. 3B). Moreover, because T98G and U87MG cells differ for the p53 status, we investigated the role of p53 in G5-induced death by producing U87MG cells expressing the hotspot mutation of p53 R175H (Fig. 3B).

Initially, we verified the ability of mutated p53 and Bcl-xL to modulate apoptosis in response to DNA damage. As recently observed (15), we confirmed that downregulation of wild-type p53 promotes death of U87MG cells in response to DNA-damaging agents. However, the introduced p53 mutant did not influence the necrotic response activated by G5 (Fig. 3C and D). Similarly, overexpressed Bcl-xL was able to reduce cell death in response to DNA damage, but it failed in counteracting G5-induced necrosis (Fig. 3C and D).
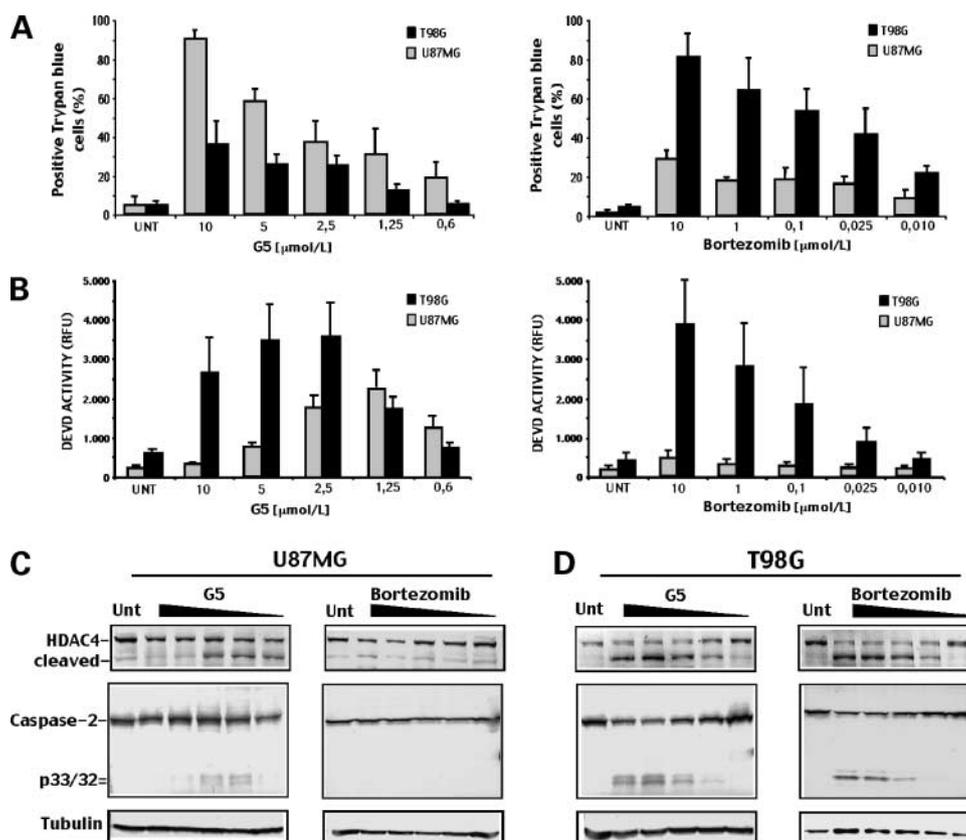
Figure 1. Cell death in GBM cells in response to G5 or bortezomib treatments. **A,** U87MG and T98G cells were treated with the indicated concentrations of G5 or bortezomib for 20 h, and the appearance of cell death was scored by trypan blue staining [*columns,* mean (*n* = 3); *bars,* SD]. **B,** caspase-3/7 (DEVDase) activity in U87MG and T98G cells treated with the indicated concentrations of G5 or bortezomib for 20 h [*columns,* mean (*n* = 3); *bars,* SD]. Processing of caspase-2 and HDAC4 in U87MG (**C**) or T98G (**D**) cells treated for 20 h with escalating concentrations of G5 or bortezomib as in **A** and **B,** respectively. Equal amounts of cell lysates were subjected to SDS-PAGE electrophoresis. Immunoblots were done using the indicated antibodies. Tubulin was used as loading control.

Figure 2. G5 but not bortezomib can activate a caspase independent necrotic death in U87MG cells. **A,** U87MG and T98G cells were treated for 20 h with the indicated concentrations of G5 or bortezomib in the presence or not of the caspase inhibitor zVAD.fmk. Cell death was scored by trypan blue staining [*columns,* mean; (*n* = 4); *bars,* SD]. *, $P < 0.05$. **B,** U87MG and T98G cells were pretreated for 1 h with CHX (1 μg/mL) and then incubated with the indicated concentration of G5. Cell death was scored 20 h later. *Columns,* mean (*n* = 5); *bars,* SD. *, $P < 0.05$. **C,** U87MG and T98G cells were treated with the indicated concentrations of G5 and DMNQ. Cell death was scored 20 h later.
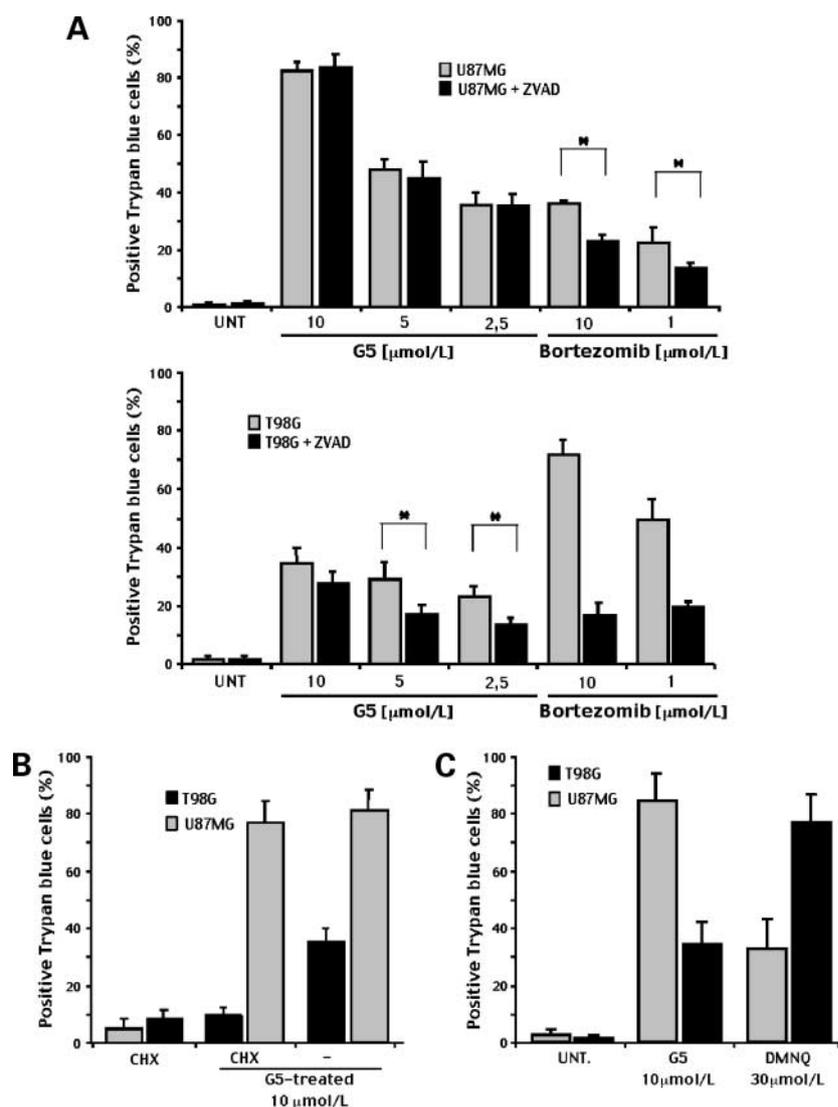


Transcriptome Analysis of U87MG and T98G Cells

To understand the gene expression basis of the divergent death responses elicited by UPSIs in U87MG and T98G cells, we compared the gene expression profiles of the two cell lines using Affymetrix GeneChip Human Genome U133A 2.0 Arrays. After statistical test, probe sets with signal intensities displaying over 2-fold difference between the two cell lines were selected. Overall, 2,522 genes appear differentially expressed between U87MG and T98G cells, thus confirming a certain degree of genetic heterogeneity in GBM cell lines, as observed in other gene expression profile studies (16). The top 20 upregulated and downregulated genes are shown in Table 1. Many of these genes point to relevant differences in the microenvironment as generated by soluble and insoluble factors secreted by the two cell lines and in the detoxification systems (see also Supplementary Tables S2–4). Although T98G and U87MG cells differ profoundly for the susceptibility to apoptosis in response to UPSIs, expression profile analysis of apoptosis regulators, including inhibitor of apoptosis cas-

pases and Bcl-2 family members, has not revealed overt differences between the two cell lines (Supplementary Table S1).

U87MG cells harbor a homozygous deletion of the entire *IFNA/IFNW* gene cluster and of the *IFNB1* gene (17). The microarray analysis confirmed that the expression of many IFN-induced genes is higher in T98G cells; however, treatment of U87MG cells with IFN-α does not influence cell death induced by G5 or bortezomib (data not shown).

Glutathione Depletion Sensitizes Gliobastoma Cells to G5-Induced Death

Genes regulating oxidative stress (*GSTM3, PXDN,* and *GPX3*) are among the 20 highest differentially expressed genes in T98G compared with U87MG cells (Table 1). We also analyzed in detail the expression levels of genes involved in glutathione (GSH) synthesis and use (Supplementary Table S2). In particular, T98G cells express higher levels of GSH transferase M3 (*GSTM3*) and of glutamate-cysteine ligase (*GCLC*) transcripts, whereas U87MG express other GSH S-transferase (GST) isoforms. Differences in the expression
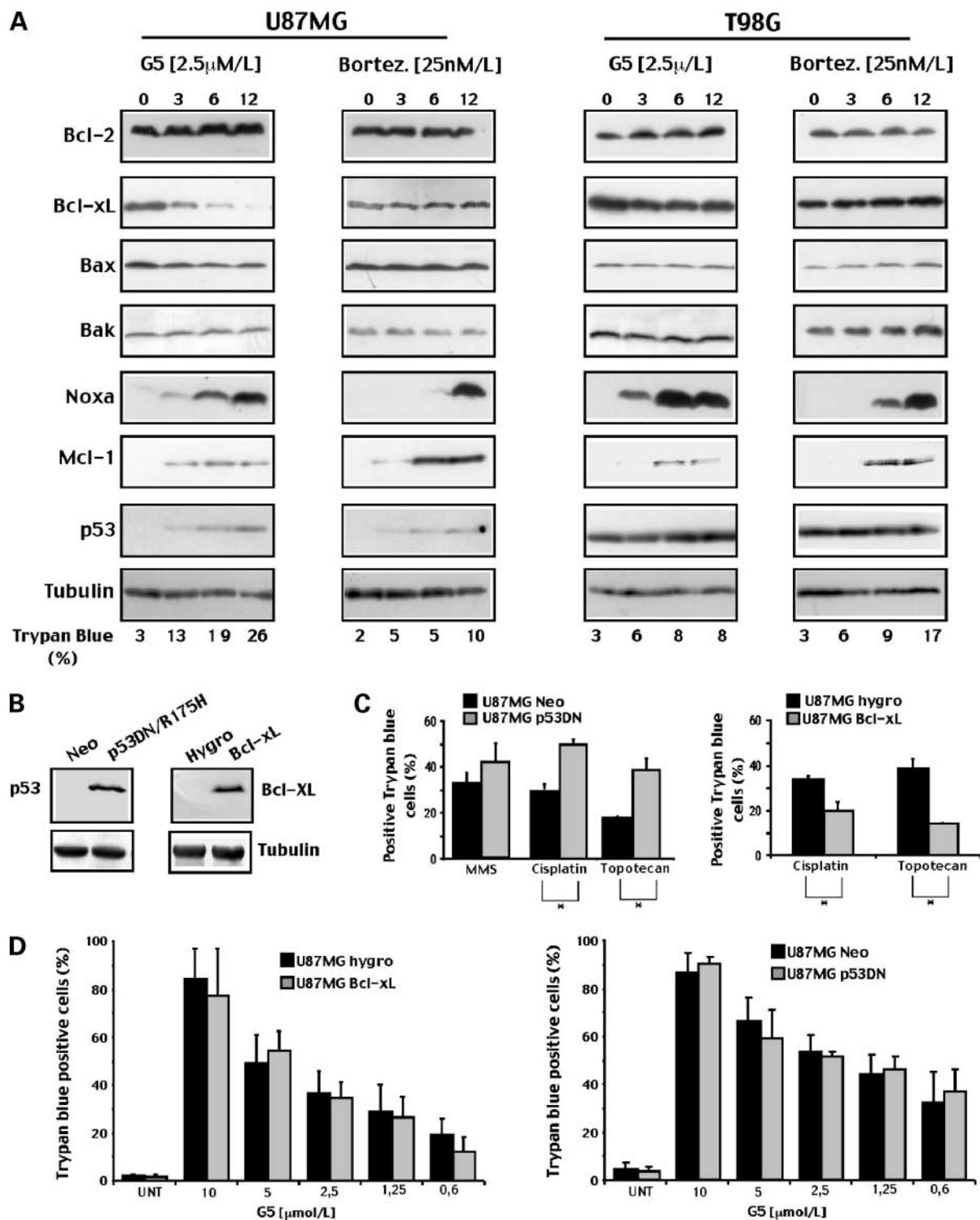
Figure 3. Regulation of Bcl-2 family member expression in GBM cells in response to G5 or bortezomib. **A,** time course analysis of the expression levels of Bcl-2 family members and p53. Lysates from U87MG and T98G cells treated with G5 or bortezomib for the indicated times were prepared and subjected to immunoblot analysis using the specific antibodies. **B,** generation of U87MG cells expressing dominant-negative p53 or Bcl-xL. Equal amounts of cellular lysates from U87MG cells expressing *bcl-xL, p53R175H,* or the relative resistance genes were subjected to SDS-PAGE electrophoresis. Immunoblots were done using the indicated antibodies. **C,** U87MG cells expressing p53R175H mutant, Bcl-xL, or the relative control genes were treated for 24 h with MMS (100 μg/mL), or for 48 h with cisplatin (250 μmol/L) or topotecan (1 μmol/L). Cell death was scored by trypan blue staining [*columns,* mean (*n* = 3); *bars,* SD]. *, *P* < 0.05. **D,** U87MG cells expressing p53R175H mutant, Bcl-xL, or the relative control genes were treated with the indicated concentrations of G5 for 20 h, and the appearance of cell death was scored by trypan blue staining [*columns,* mean (*n* = 3); *bars,* SD].

Table 1. **Top 20 upregulated and top 20 downregulated genes in T98G cells relative to U87MG cells**

Gene symbol	Fold difference*	Gene name	Function	Localization	ProbeSet ID	*P*
IGFBP5	8,64	Insulin-like growth factor binding protein 5	Signaling	Secreted	211959_at	6,20E-09
CDH6	7,89	Cadherin 6, type 2, K-cadherin (fetal kidney)	Adhesion	Plasma membrane	205532_s_at	1,53E.-08
THBS1	7,88	Thrombospondin 1	Adhesion/signaling	Secreted/ECM	201109_s_at	2.30E-08
CDH11	7,38	Cadherin 11, type 2, OR-cadherin (osteoblast)	Adhesion	Plasma membrane	207173_x_at	7,51E-08
TNFRSF11B	6,83	Tumor necrosis factor receptor superfamily, member 11b	Signaling	Secreted	204933_s_at	2,3OE-08
GSTM3	6,81	GST M3 (brain)	Redox	Intracellular	202554_s_at	2,30E-08
CXCL12	6,70	Chemokine(C-X-Cmotif) ligand 12 (stromal cell–derived factor 1)	Signaling	Secreted	209687_at	5,85E-08
GPX3	6,64	Glutathione peroxidase 3 (plasma)	Redox	Secreted	201348_at	9.93E-09
MYH10	6,51	Myosin, heavy chain 10, nonmuscle	Cytoskelelon	cytoplasmic	212372_at	3,52E-06
PDGFD	6,44	Platelet-derived growth factor D	Signaling	Secreted	219304_s_at	7,71E-08
COLEC12	6,31	Collectin subfamily member 12	Host defense	Plasma membrane	221019_s_at	7,51E-08
PXDN	6,26	Peroxidasin homologue (Drosophila)	Redox	Secreted/ECM	212013_at	2.13E-08
HSPA1A	6,25	Heat shock 70 kDa protein 1A	Chaperon	Intracellular	200799_at	2,30E-08
SLC2A10	6,23	Solute currier family 2 (facilitated glucose transporter), member 10	Transport	Plasma membrane	221024_s_at	3,98E-07
NIDI	6,18	Nidogen 1	Adhesion	Secreted/ECM	202007_at	7,51E-08
TUSC3	6,10	Tumor suppressor candidate 3	N-Glycosylation	ER	213423_x_at	2,30E-08
RHBDL2	6,07	Rhomboid, veinlet-like 2 (Drosophila)	Signaling	Plasma membrane	219489_s_at	7,67E-08
GABRA2	5,92	γ-Aminobutyric acid (GABA) A receptor, α 2	Ion transport	Plasma membrane	207014_at	2,77E-06
CYTL1	5,84	Cytokine-like 1	Signaling	Secreted	219837_s_at	1,53E-08
NPTX1	5,78	Neuronal pentraxin I	Synaptic transmission	Intracellular	204684_at	5,82E-08
EREG	−8,27	Epiregulin	Signaling	Secreted	205767_at	3,14E-08
GREM1	−7,90	Gremlin 1, cysteine knot superfamily, homologue (*Xenopus* laevis)	Signaling	Secreted	218468_s_at	7,68E-08
PRSS7	−7,38	Protease, serine, 7 (enterokinase)	Proteolysis	Plasma Membrane	207638_at	5,39E-08
FABP5	−7,22	Fatty acid binding protein 5 (psoriasis associated)	Transport	Cytoplasmic	202345_s_at	1,57E-08
NETO2	−6,91	Neuropilin (NRP) and tolloid (TLL)-like 2	Signaling?	Plasma Membrane	218888_s_at	5,32E-08
NRIP3	−6,73	Nuclear receptor interacting protein 3	Unknown	Unknown	219557_s_at	5.82E-08
ETVl	−6,62	Ets variant gene 1	Trancription	Nuclear	221911_at	7,68E-08
C3orf14	−6,42	Chromosome 3 open reading frame 14	Unknown	Unknown	219288_at	8,02E-08
SVIL	−6,41	Supervillin	Cytoskeleton	Plasma Membrane	202565_s_at	373E-08
PLAGL1	−5,86	Pleiomorphic adenoma gene-like 1	Trancription	Nuclear/Cytoplasm.	209318_x_at	1.11E-06
PKIA	−5,67	Protein kinase (CAMP-dependent, catalytic) inhibitor α	Signaling	Nuclear/Cytoplasm.	204612_at	2,55E-08
MCTP1	−5,65	Multiple C2 domains, transmembrane 1	Unknown	Plasma Membrane	220122_at	8.54E-07

(Continued on the following page)

Table 1. Top 20 upregulated and top 20 downregulated genes in T98G cells relative to U87MG cells (Cont'd)

Gene symbol	Fold difference*	Gene name	Function	Localization	ProbeSet ID	P
MYO1B	−5,64	Myosin IB	Cytoskeleton	Cytoplasmic	212364_at	167E-07
HGF	−5,55	Hepatneyte growth factor (hepapoietin A; scatter factor)	Signaling	Secreted	210997_at	2,55E-08
ABCA1	−5,50	ATP-binding cassette, subfamily A (ABC1), member 1	Transport	Plasma Membrane	203504_s_at	5.94E-08
AHNAK2	−5,47	AHNAK nucleoprotein 2	Transport	Secreted	212992_at	8,35E-08
PLTP	−5,45	Phospholipid transfer protein	Scaffolding	Nuclear/Cytoplasm.	202075_s_at	8,29E-08
PRRX1	−5,38	Paired related homeobox 1	Trancription	Nuclear	205991_s_at	1,13E-07
HS3ST3A1	−5,35	Heparan sulfate (glucosamine) 3-O-sulfotransferase 3A1	ECM modifier	Plasma Membrane	219985_at	6,19E-08
UGT8	−5,34	UDP glycosyltransferase 8	Sphingolipids biosynth.	ER	208358_s_at	3,43E-07

*(log2) − mean fold differences.

levels of the GST enzymes were also confirmed by affinity purification and by measuring enzymatic activities (Supplementary Fig. S2).

GSTs are crucial enzymes in the detoxification process, catalyzing the nucleophilic attack of GSH on toxic electrophilic substrates (18). *De novo* GSH synthesis is governed by γ-glutamylcysteine synthetase, a heterodimer constituted by a catalytic subunit (GCLC) and a modulatory subunit (GCLM; ref. 19).

The GSH system can modulate chemoresistance (20, 21); hence, differential detoxification abilities between the two cell lines could explain the resistance to G5-dependent necrosis observed in T98G cells. To answer this question, cells were depleted of GSH, by pretreatment with buthionine sulfoximine (BSO), a selective inhibitor of γ-glutamylcysteine synthetase (22). The appearance of death was then analyzed in response to G5 or bortezomib.

As shown in Fig. 4A, in agreement with previous studies (23), GSH depletion does not induce cell death. However, when GSH-depleted cells were treated with G5, cell death was similarly augmented in T98G and U87MG cells. On the contrary, cell death induced by bortezomib was unaffected by BSO treatment.

Next, we evaluated whether the death of T98G cells in the presence of BSO was still caspase dependent. As shown in Fig. 4B, in response to 2.5 μmol/L of G5, death of T98G cells was caspase dependent, whereas at 10 μmol/L, it was largely caspase independent. Caspase inhibitors failed to block apoptosis induced by 2.5 μmol/L of G5 when BSO was present. As observed in other models (24), caspase inhibitors augmented necrosis in response to 10 μmol/L of G5, possibly by suppressing autophagy (25). Finally, as described before (Fig. 2), death of U87MG was largely caspase independent.

The Extracellular Environment Modulates the Susceptibility to Necrosis

The most prominent group of highly differential expressed genes between U87MG and T98G cells comprises components of the microenvironment, including elements of the ECM (Supplementary Tables S3 and S4; Table 1). Transcripts for thrombospondin (*THBS1*), collagen type III, IV, and XVIII (*CL3A1, COL18A1,* and *COL4A1*) are the top highest expressed ECM components in T98G cells (Supplementary Table S4). Transcripts for osteopontin (*SPP1*), mesotypsin (*PRRS3*), tenascin C (*TNC*), and collagen I (*COL1A*) are the top highest expressed ECM components in U87MG cells (Supplementary Table S3). Differential expression of TNC and collagen IV in U87MG and T98G cells was validated at protein levels (Fig. 5A and B).

We have recently shown that ECM components collagen and fibronectin can counteract G5-dependent necrosis (11). Therefore, different types of ECM, as produced by the GBM cell lines, could influence the susceptibility to G5-induced necrosis. To answer this question, U87MG and T98G cells were plated on fibronectin, collagen IV, or on bovine serum albumin–coated Petri dishes and next treated with G5.

Figure 5C illustrates that collagen IV and fibronectin can counteract the necrotic response to G5 in U87MG cells. An ∼40% reduction in necrosis is manifested by both ECM components in U87MG cells treated for 24 hours with 10 μmol/L of G5. Death of T98G cells was less influenced by fibronectin and collagen IV (Fig. 5D), presumably because it is also apoptotic. An ∼30% reduction with collagen IV and a 22% reduction with fibronectin were observed in the presence of high concentrations of G5.

Discussion

Apoptosis and necrosis represent the most common forms of cell death. Traditionally, apoptosis is considered a form of regulated cellular mechanism in contrast to necrosis, which is described as a form of passive death. Necrosis appears when cells suffer excessive stresses that finally cause the rupture of the plasma membrane and the spillage of cellular macromolecules, which act as proinflammatory signals (26, 27). More recent data have challenged this view and the existence of regulated forms of necrosis is becoming evident (27, 28).

Figure 4. GSH depletion modulates cell death in response to G5 and the apoptotic/necrotic switch. **A,** U87MG or T98G cells were pretreated with BSO for 24 h. Next, G5 or bortezomib were added for further 24 h. Cell death was scored by trypan blue staining [*columns,* mean (*n* = 3); *bars,* SD]. *, *P* < 0.05. **B,** U87MG or T98G cells were pretreated with BSO for 24 h followed by 1 h of pretreatment with zVAD.fmk (100 μmol/L). Next, G5 or bortezomib was added for further 24 h as indicated. Cell death was scored by trypan blue staining [*columns,* mean (*n* = 3); *bars,* SD]. *, *P* < 0.05.
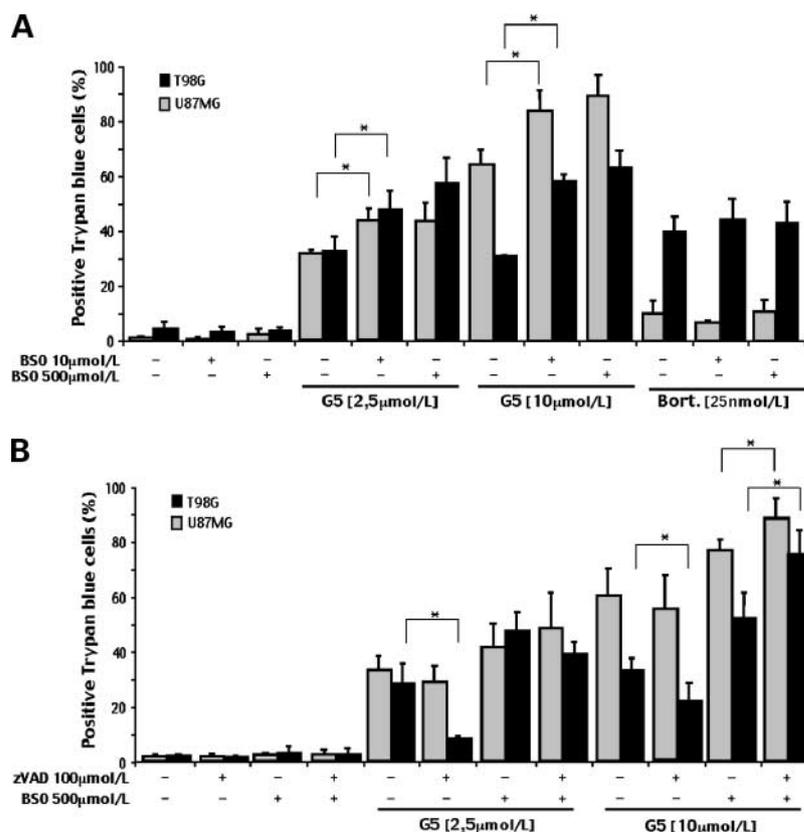
Apoptosis

U87MG cells show resistance to apoptosis but they are susceptible to die by G5-induced necrosis. In contrast, T98G cells are susceptible to die by apoptosis in response to both inhibitors but show some resistance to G5-induced necrosis. Interestingly, a difference in the apoptotic response to bortezomib, between these cell lines, can also be appreciated from previous studies (29, 30).

Our data do not disclose robust alterations in the expression or modulation of components of the apoptotic machinery between T98G and U87MG cells. Bax and Bak, which are necessary for apoptosis in response to UPSIs (11), are similarly expressed in the two cell lines. Noxa and Mcl-1, two Bcl-2 family members under the regulation of UPSIs, are alike induced by the two insults. Moreover, expression profile studies did not evidence overt differences in the expression levels of Bcl-2 family members, caspases, and inhibitors of apoptosis. Moreover, we noted that bortezomib failed to induce mitochondrial outer membrane permeabilization in U87MG cells.[3] Hence, it is possible that other mechanisms, acting upstream of mitochondria, are responsible for the divergences in the apoptotic responsiveness.

Necrosis

U87MG cells are susceptible to G5-induced necrosis, whereas T98G cells show some resistance. This necrotic

susceptibility was specific for G5. In fact, in response to oxidative stress, T98G cells were more prone to die by necrosis compared with U87MG cells, thus ruling out that U87MG cells are in general more susceptible to necrosis. This observation indicates that cells can activate different necrotic responses.

G5 triggers the upregulation of wild-type p53 and downregulation of Bcl-xL in U87MG cells. However, neither of these two proteins can modulate the necrotic response to G5.

Combining expressional profile studies and functional studies has permitted to disclose that differences in the necrotic responsiveness could arise from diversity in the GSH detoxification system and in the microenvironment and, in particular, in the type of ECM proteins.

U87MG and T98G cells differ profoundly for the classes of GST enzymes expressed. *GSTM3* is abundantly expressed in T98G cells, and also, the γ-glutamylcysteine synthetase is expressed at higher levels in this cell line. Depletion experiments have indicated that GSH can modulate at least two events: (*a*) the rate of cell death in response to G5, possibly by G5 detoxification, (*b*) the decision about the particular type of death in response to G5, necrosis versus apoptosis.

Depending on the cellular context and the death insult, GSH depletion can synergize to induce apoptosis, necrosis, or can also switch the mode of death versus necrosis (20, 31, 32). GSH depletion can generate reactive oxygen species, increase the irreversible oxidation of cysteine residues,

---

[3] C. Foti, unpublished observation.

and can also influence the formation of protein-GSH mixed disulphides (*S*-glutathionylation; ref. 23). However, because the cotreatment with BSO and G5 failed to elicit oxidative damage in T98G cells (Supplementary Fig. S2C), something different from ROS generation should be evoked to explain the shift toward necrosis.

Interestingly, recent data have shown that *S*-glutathionylation of Fas increases its accumulation in lipid rafts and strengthens the death signal (33). Because G5 engages the extrinsic pathway to induce apoptosis (8, 11), we hypothesize that a reduction in *S*-glutathionylation of Fas could promote the appearance of necrosis in T98G cells treated with G5.

We also found that the microenvironment, as generated through the secretion of ECM components, differs profoundly between T98G and U87MG cells.

Interestingly, gene expression profile studies in brain tumors in comparison with normal brain tissue have revealed that GBMs overexpress genes of the microenvironment,

including growth factor–related and structural/ECM-related genes (34–36). Differences in the microenvironment mark also different subtypes of GBMs. Primary GBMs with respect to secondary GBMs express genes characteristic of mesenchymal-derived tissues and stromal response (36, 37).

Among ECM genes highly expressed in the necrosis-resistant T98G cells, a consistent group was also identified as more expressed in primary GBM compared with normal brain tissue (38). This list includes *COL3A1*, *COL4A1*, *POSTN*, *COL4A2*, *LAMB1*, and *MGP* (38). *COL4A1* and *COL4A2* were also more expressed in primary GBMs with respect to secondary GBMs (36, 37). On the contrary, this list was extremely reduced in U87MG cells including only *TNC* and *TIMP1* genes.

Protection from G5-induced necrosis can be elicited in U87MG cells after adhesion to ECM. Adhesion to collagen IV, which is more expressed in T98G cells or to exogenous-added fibronectin, significantly rescued cells from death. It
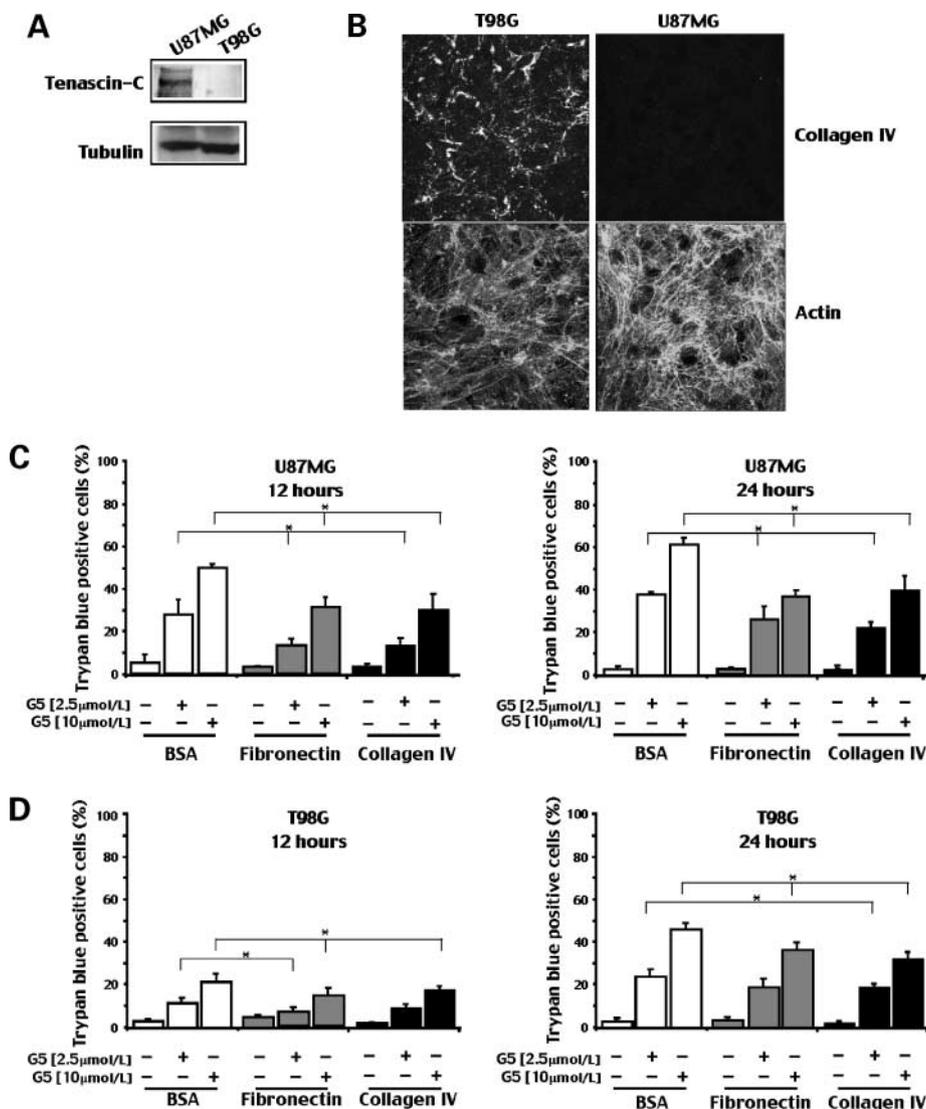
Figure 5. The microenvironment regulates the susceptibility to G5-induced necrosis. **A,** lysates from U87MG and T98G cells were prepared and subjected to immunoblot analysis using anti–tenascin-C antibody. Anti-tubulin was used as loading control. **B,** confocal microscopic analysis of U87MG and T98G cells 96 h after plating using rabbit anti–collagen IV antibody. The immunocomplexes were visualized with an anti-rabbit FITC-conjugated antibody and actin filaments with phalloidin-TRITC. Deposition of collagen IV can be visualized only in T98G cells. **C,** U87MG or (**D**) T98G cells were grown on fibronectin, collagen IV, or bovine serum albumin (*BSA*) as indicated. Six hours after seeding, cells were incubated with G5 (2.5 or 10 μmol/L) for 12 or 24 h. Cell death was scored by trypan blue staining [*columns,* means (n = 3); *bars,* SD]. *, $P < 0.05$.

is important to note that, although tenascin C (Tnc) enhances proliferation of glioma cells, it also inhibits cell spreading on fibronectin (39). This effect explains the antinecrotic role of exogenously added fibronectin, which can compete with the high levels of Tnc secreted by U87MG cells to promote adhesion. A role confirmed after the downregulation of Tnc expression by siRNA transfection, which, similarly to fibronectin addition, reduced G5-induced necrosis in U87MG cells (Supplementary Fig. S3).

We have recently shown that G5 can trigger necrosis in apoptotic-resistant cells (11). This necrotic death was likewise inhibited by adhesion to ECM. G5-induced necrosis was independent from common necrotic regulators such as oxidative stress, calcium, c-Jun-NH$_2$-kinase, and RIP1. Instead, it is characterized by an early and dramatic reorganization of actin cytoskeleton. We have similarly noted that G5 triggers dramatic changes in actin organization in U87MG but not in T98G cells. Before the appearances of necrotic markers, cells reduce actin projections, become polygonal, and next, with time, they eventually round up and detach (see Supplementary Fig. S4). The impact of G5 on actin dynamics and cell adhesion was corroborated by the diminished random migration scored in U87MG cells treated with low doses of G5 (see Supplementary Fig. S5). In the future, to define this necrotic pathway in more detail, it will be important to exclude off-target effects of G5, possibly through the development of more specific isopeptidase inhibitors.

Necrotic deaths that rely on microfilament/adhesion changes, as in the case of G5, have been recently observed (40). Necrotic death of lymphocytes, in response to mycophenolic, which involves Rho-GTPase Cdc42 activity and actin polymerization, shares some features with G5. In fact, it is Bcl-2, c-Jun-NH$_2$-kinase, and RIP independent (41).

Despite aggressive approaches, treatment of GBM patients represents an ongoing challenge (1, 2). Characterization of new necrotic pathways is important to overcome the resistance to apoptosis typical of GBMs. In addition, considering the necrotic propensity of GBMs, understanding the molecular mechanisms that govern necrosis is instrumental to design new therapeutic treatments. By characterizing the death response of GBM cell lines to G5 and bortezomib, we have provided a contribution to these important issues.

Disclosure of Potential Conflicts of Interest

No potential conflicts of interest were disclosed.

References

1. Furnari FB, Fenton T, Bachoo RM, et al. Malignant astrocytic glioma: genetics, biology, and paths to treatment. Genes Dev 2007;21:2683–710.

2. Zhu Y, Parada LF. The molecular and genetic basis of neurological tumours. Nat Rev Cancer 2002;2:616–26.

3. Demarchi F, Brancolini C. Altering protein turnover in tumor cells: new opportunities for anti-cancer therapies. Drug Resist Updat 2005; 8:359–68.

4. Brancolini C. Inhibitors of the ubiquitin-proteasome system and the cell death machinery: how many pathways are activated? Curr Mol Pharm 2008;1:24–37.

5. Love KR, Catic A, Schlieker C, Ploegh HL. Mechanisms, biology and inhibitors of deubiquitinating enzymes. Nat Chem Biol 2007;3: 697–705.

6. Amerik AY, Hochstrasser M. Mechanism and function of deubiquitinating enzymes. Biochim. Biophys Acta 2004;1695:189–207.

7. Kirkin V, Dikic I. Role of ubiquitin- and Ubl-binding proteins in cell signaling. Curr Opin Cell Biol 2007;19:199–205.

8. Aleo E, Henderson CJ, Fontanini A, Solazzo B, Brancolini C. Identification of new compounds that trigger apoptosome-independent caspase activation and apoptosis. Cancer Res 2006;66:9235–44.

9. Mullally JE, Fitzpatrick FA. Pharmacophore model for novel inhibitors of ubiquitin isopeptidases that induce p53-independent cell death. Mol Pharmacol 2002;62:351–8.

10. Nicholson B, Leach CA, Goldenberg SJ, et al. Characterization of ubiquitin and ubiquitin-like-protein isopeptidase activities. Protein Sci 2008; 17:1035–43.

11. Fontanini A, Foti C, Potu H, et al. The isopeptidase inhibitor G5 triggers a caspase-independent necrotic death in cells resistant to apoptosis: a comparative study with the proteasome inhibitor bortezomib. J Biol Chem 2009;284:8369–81.

12. Henderson CJ, Aleo E, Fontanini A, Maestro R, Paroni G, Brancolini C. Caspase activation and apoptosis in response to proteasome inhibitors. Cell Death Differ 2005;12:1240–54.

13. Opel D, Westhoff MA, Bender A, Braun V, Debatin KM, Fulda S. Phosphatidylinositol 3-kinase inhibition broadly sensitizes glioblastoma cells to death receptor- and drug-induced apoptosis. Cancer Res 2008; 68:6271–80.

14. Fischer U, Janicke RU, Schulze-Osthoff K. Many cuts to ruin: a comprehensive update of caspase substrates. Cell Death Differ 2003; 10:76–100.

15. Batista LF, Roos WP, Christmann M, Menck CF, Kaina B. Differential sensitivity of malignant glioma cells to methylating and chloroethylating anticancer drugs: p53 determines the switch by regulating xpc, ddb2, and DNA double-strand breaks. Cancer Res 2007;67:11886–95.

16. Li A, Walling J, Kotliarov Y, et al. Genomic changes and gene expression profiles reveal that established glioma cell lines are poorly representative of primary human gliomas. Mol Cancer Res 2008;6:21–30.

17. Olopade OI, Jenkins RB, Ransom DT, et al. Molecular analysis of deletions of the short arm of chromosome 9 in human gliomas. Cancer Res 1992;52:2523–9.

18. Hayes JD, Flanagan JU, Jowsey IR. Glutathione transferases. Annu Rev Pharmacol Toxicol 2005;45:51–88.

19. Dickinson DA, Levonen AL, Moellering DR, et al. Human glutamate cysteine ligase gene regulation through the electrophile response element. Free Radic Biol Med 2004;37:1152–9.

20. Troyano A, Fernández C, Sancho P, De Blas E, Aller P. Effect of glutathione depletion on antitumor drug toxicity (apoptosis and necrosis) in U-937 human promonocytic cells. The role of intracellular oxidation. J Biol Chem 2001;276:47107–15.

21. Syng-Ai C, Kumari AL, Khar A. Effect of curcumin on normal and tumor cells: role of glutathione and bcl-2. Mol Cancer Ther 2004;3:1101–8.

22. Griffith OW, Meister A. Potent and specific inhibition of glutathione synthesis by buthionine sulfoximine (S-n-butyl homocysteine sulfoximine). J Biol Chem 1979;254:7558–60.

23. Di Stefano A, Frosali S, Leonini A, et al. GSH depletion, protein S-glutathionylation and mitochondrial transmembrane potential hyperpolarization are early events in initiation of cell death induced by a mixture of isothiazolinones in HL60 cells. Biochim Biophys Acta 2006;1763:214–25.

24. Vercammen D, Beyaert R, Denecker G, et al. Inhibition of caspases increases the sensitivity of L929 cells to necrosis mediated by tumor necrosis factor. J Exp Med 1998;187:1477–85.

25. Wu YT, Tan HL, Huang Q, et al. Autophagy plays a protective role during zVAD-induced necrotic cell death. Autophagy 2008;4:457–66.

26. Golstein P, Kroemer G. Cell death by necrosis: towards a molecular definition. Trends Biochem Sci 2007;32:37–43.

27. Zong WX, Thompson CB. Necrotic death as a cell fate. Genes Dev 2006;20:1–15.

28. Hitomi J, Christofferson DE, Ng A, et al. Identification of a molecular signaling network that regulates a cellular necrotic cell death pathway. Cell 2008;135:1311–23.

29. Yin D, Zhou H, Kumagai T, et al. Proteasome inhibitor PS-341 causes cell growth arrest and apoptosis in human glioblastoma multiforme (GBM). Oncogene 2005;24:344–54.

30. La Ferla-Bruhl K, Westhoff MA, Karl S, et al. NF-kB-independent sensitization of glioblastoma cells for TRAIL-induced apoptosis by proteasome inhibition. Oncogene 2007;26:571–82.

31. Fernandes RS, Cotter TG. Apoptosis or necrosis: intracellular levels of glutathione influence the mode of cell death. Biochem. Pharmacol 1994; 48:675–81.

32. Chen D, Chan R, Waxman S, Jing Y. Buthionine sulfoximine enhancement of arsenic trioxide-induced apoptosis in leukemia and lymphoma cells is mediated via activation of c-Jun NH2-terminal kinase and up-regulation of death receptors. Cancer Res 2006;66:11416–23.

33. Anathy V, Aesif SW, Guala AS, et al. Redox amplification of apoptosis by caspase-dependent cleavage of glutaredoxin 1 and S-glutathionylation of Fas. J Cell Biol 2009;184:241–52.

34. Ljubimova JY, Lakhter AJ, Loksh A, et al. Overexpression of α4 chain-containing laminins in human glial tumors identified by gene micro-array analysis. Cancer Res 2001;61:5601–10.

35. Freije WA, Castro-Vargas FE, Fang Z, et al. Gene expression profiling of gliomas strongly predicts survival. Cancer Res 2004;64:6503–10.

36. Phillips HS, Kharbanda S, Chen R, et al. Molecular subclasses of high-grade glioma predict prognosis, delineate a pattern of disease progression, and resemble stages in neurogenesis. Cancer Cell 2006;9:157–73.

37. Tso CL, Freije WA, Day A, et al. Distinct transcription profiles of primary and secondary glioblastoma subgroups. Cancer Res 2006;66:159–67.

38. Tso CL, Shintaku P, Chen J, et al. Primary glioblastomas express mesenchymal stem-like properties. Mol Cancer Res 2006;4:607–19.

39. Huang W, Chiquet-Ehrismann R, Moyano JV, Garcia-Pardo A, Orend G. Interference of tenascin-C with syndecan-4 binding to fibronectin blocks cell adhesion and stimulates tumor cell proliferation. Cancer Res 2001;61:8586–94.

40. Belkaid A, Fortier S, Cao J, Borhane A. Necrosis induction in glioblastoma cells reveals a new "bioswitch" function for the MT1-MMP/G6PT signaling axis in proMMP-2 activation versus cell death decision. Neoplasia 2007;9:332–40.

41. Chaigne-Delalande B, Guidicelli G, Couzi L, et al. The immunosuppressor mycophenolic acid kills activated lymphocytes by inducing a nonclassical actin-dependent necrotic signal. J Immunol 2008;181:7630–8.

Molecular Cancer Therapeutics

Characterization of caspase-dependent and caspase-independent deaths in glioblastoma cells treated with inhibitors of the ubiquitin-proteasome system

Carmela Foti, Cristina Florean, Antonio Pezzutto, et al.

Updated version	Access the most recent version of this article at: doi:10.1158/1535-7163.MCT-09-0431
Supplementary Material	Access the most recent supplemental material at: http://mct.aacrjournals.org/content/suppl/2009/12/15/1535-7163.MCT-09-0431.DC1

Cited articles	This article cites 41 articles, 21 of which you can access for free at: http://mct.aacrjournals.org/content/8/11/3140.full#ref-list-1
Citing articles	This article has been cited by 1 HighWire-hosted articles. Access the articles at: http://mct.aacrjournals.org/content/8/11/3140.full#related-urls

E-mail alerts	Sign up to receive free email-alerts related to this article or journal.
Reprints and Subscriptions	To order reprints of this article or to subscribe to the journal, contact the AACR Publications Department at pubs@aacr.org.
Permissions	To request permission to re-use all or part of this article, use this link http://mct.aacrjournals.org/content/8/11/3140. Click on "Request Permissions" which will take you to the Copyright Clearance Center's (CCC) Rightslink site.